WIBECAM: Device Free Human Activity Recognition Through WiFi Beacon-Enabled Camera

Mauro De Sanctis, Ernestina Cianca, Simone Di Domenico, Daniele Provenziani, Giuseppe Bianchi, Marina Ruggieri
Dept. of Electronic Engeneering, University of Rome Tor Vergata
Rome, Italy
mauro.de.sanctis@uniroma2.it, ernestina.cianca@uniroma2.it, simone.di.domenico@uniroma2.it, giuseppe.bianchi@uniroma2.it

ABSTRACT

This paper presents WIBECAM, a Human Activity Recognition system which does not require neither user instrumentation, nor specialized infrastructure, nor active operation - it passively leverages Beacon frames periodically emitted by a single off-the-shelf Wi-Fi access point. As many other recent proposals, WIBECAM also exploits the different multipath conditions (and their temporal variations) induced by human activity. In most of the previously proposed systems, the classification is based on the characterization of the signal strength variations, caused by the human activity. WIBECAM's main distinguishing aspect is that it "watches" the channel in the frequency domain where spectral metrics, calculated on the raw signal samples of the received Beacon frames, are like "snapshots" of the channel taken in a regular and periodical way. The classification process uses properly selected features that measure the changes of consecutive "snapshots". WIBECAM adapts to any Wi-Fi access point (and may comply even with legacy 802.11b-only ones), as it does not exploit neither OFDM and CSI extracted from the receiver, nor MIMO/multiple antennas. WIBECAM has been built into USRP software radios. Its classification accuracy has been preliminarily assessed for four different activities in two different environments; the resulting confusion matrices show very promising performance.

Categories and Subject Descriptors

H.4 [**Information Systems Applications**]: Miscellaneous

Keywords

Device-free Human Activity Recognition, WiFi, RF sensing.

1. INTRODUCTION

This paper presents WIBECAM, an Activity Recognition (AR) system that requires neither user instrumentation nor an infrastructure of cameras. The WIBECAM system makes use of a single Access Point (AP) and a single WiFi receiver with single antennas, in contrast with other recent AR systems that use multiple receivers and/or multiple APs and/or multiple antennas (e.g. [1], [2]). As several other recently proposed AR systems [1], [3], WIBECAM captures WiFi signals in an environment by looking at multi-path distortions or, more precisely, their time variations which are related to human motion in the environment. Key elements of the proposed AR systems are a) use of the Beacon messages of a WiFi AP; b) extraction of the channel frequency behavior from the I/Q components of the received signal; c) a videocamera-like approach for automatic AR to catch the time variations of the channel frequency behavior.

Use of beacon signals - Our AR system collects the raw signal samples from the Beacon packets of just *a single* AP. The advantages of using Beacon packets, instead of data packets [4], are manyfold:

1. No need to transmit or receive user-generated data from the AP (hence no waste of channel resources).
2. In contrast with AR systems that require a continuous transmission, we proved that our system can effectively use short length data packets (the Beacon messages) with long inactive periods in the order of tens of ms.
3. No need to authenticate to the AP.
4. It can be applied to any IEEE802.11x standard, including Orthogonal Frequency Division Multiplexing (OFDM) standards and non-OFDM standards.

As shown in Section II, other works also use Beacon messages, but in a different way [2].

Channel behaviour in the frequency domain - The proposed system uses the raw signal samples of the received Beacon packets to calculate the channel behavior in the frequency domain, which is strictly related to the multipath propagation and hence, to the specific scatterers present in the sensed environment. We further show that the usage of estimated Power Spectral Density (PSD) is a better approach over Discrete Fourier Transform (DFT).

Videocamera-like approach - In a videocamera-based AR system, the videocamera captures images at a constant rate of about 15-30 frames per second (fps) and the automatic AR is based on the analysis of the differences between consecutive captured images. WIBECAM performs the activity recognition by capturing the frequency behavior of the channel, through specific curves (i.e. PSD), at a constant rate

WPA'15, May 22, 2015, Florence, Italy.

DOI: http://dx.doi.org/10.1145/2753497.2753499.

of $1/BI$ fps, where BI is the Beacon Interval. Then, AR is performed by properly assessing the differences among consecutive "images" of the channel in the frequency domain. Figure 1 shows the estimated PSD associated to 4 different activities. From Fig. 1 it is evident that the PSD could be used to distinguish the considered different activities. In fact, for each activity we can identify a different "shape" of the curve and a different variation of curves over the time. We have then identified the best metrics that can be used to distinguish the different "shape" and variation of the estimated curves related to the channel in the frequency domain.

The paper is organized as follows. Section II presents the most related works. Section III presents the WIBECAM system. In particular, the theoretical background, feature extraction, feature selection and classification processes are presented. Section IV shows the experimental results in terms of confusion matrices for different environments. Finally, conclusions are drawn in Section V.

2. RELATED WORKS

Human Activity Recognition Approaches are broadly classified into three categories: i) Device-Bound (DB) systems, which rely on wearable sensors (GPS, accelerometer, etc.); ii) Device-Free Active (DFA) systems, which do not require any specific user cooperation, and employ a dedicated transmitter for detection (radar [6], radio tomographic imaging, RF channel measurements, etc), and iii) Device-Free Passive (DFP) systems [5], which do not involve any active probing or signals, but exploit opportunity RF signals (WiFi, cellular 2G/3G/4G, DVB-T, FM analog radio, etc.) or natural signals (visible light, infrared, ultrasonic, etc.) cameras. Since our work falls into the RF-based DFP category, in what follows we limit to review relevant work in this area.

2.1 RF-based DFP Approaches

The concept of RF-based DFP activity recognition stems from the work published in [5]. Different DFP RF sensing AR systems are based on the observation on how some characteristic of the propagation channel varies due to human activity. These characteristics can be analyzed starting from one of the following measurements, [7]:

1. Received Signal Strength (RSS): the Received Signal Strength Indicator (RSSI) is a dimensionless quantity for RSS, which represents the signal strength observed at the receiver's antenna.

2. Channel State Information (CSI): except IEEE802.11b which is based on Direct Sequence Spread Spectrum (DS-SS), IEEE802.11x transmission is based on the use of OFDM where data symbols are sent over N orthogonal subcarriers. WiFi receivers use an estimation of Channel Frequency Response (CFR) to equalize the channel and adapt transmission parameters using the CFR as a kind of CSI. A particular driver was developed for Intel card 5300 in order to make available the CSI to computer applications [8].

3. Raw Received Signal Samples (RRSS): in this approach, the receiver collects the raw signal samples either continuously or for specific data packets. Then the RRSS are processed to extract useful features for activity classification purposes. It is worth noting that, RRSS allows to extract any given feature from the received signal, increasing the degree of freedom in the feature selection process. This approach can be applied to any RF system since it does not require to use a standard that foresees the CSI or RSS computation.

Several works on AR are based on RSS measurements. Several statistical analysis of RSS variations have been proposed to recognize different activities [9], [10]. However, this is a coarse-grained indicator for what concerns the type of activity and the recognition accuracy largely depends on the human/receiver distance [11].

On the other hand, histograms obtained from the CSI can be considered a finer-grained indicator with respect to RSS. WiFall, a device-free fall detection system which takes advantages of the CSI is presented in [3]. They obtain one value from each CSI by averaging over a subset of subcarriers and also averaging over with a number of previous values. Experimental results show that WiFall can achieve an acceptable detection and false alarm rate.

In [2] the authors propose to utilize a CSI-based correlation matrix, then obtain the eigenvalues and finally estimates the human motion according to the eigenvalue variety. This system was tested to discriminate only static or dynamic environments. The experiments carried out in this work make use of the CSI measured from Beacon messages. In their setting, there are several pairs of APs and receivers, each equipped with multiple antennas.

E-eyes system [1] applies matching algorithms to compare the CSI measurements against known profile distributions to identify the activity. Extensive experiments in two different-sized apartments have been carried out considering a large set of different activities with very good accuracy. However, such performance are achieved with several WiFi receivers.

In [12], DFP RF sensing of activities was carried out using the RRSS of the signal received from FM radio stations. The presented results, while not achieving high accuracies, refer to activities that are performed within 2.2 m from the receiver.

The WiSee system presented in [4] show that it can identify and classify a set of nine gestures with an average accuracy of 94% by extracting the micro Doppler shift from WiFi signals. The extraction of micro Doppler shift requires an observation time of 1s which is greater than the typical duration of a WiFi data packet.

Authors of [13] show that Wi-Fi can be used to see moving objects through walls and behind closed doors. In particular, the presented WiVi system identifies the number of people in a closed room and their relative locations.

In WIBECAM, for the first time, we exploit the RRSS of WiFi Beacon messages for DFP activity recognition. Moreover, in most of the previous systems the classification is based on the observation of the channel variations in the time domain while WIBECAM "watches" the channel in the frequency domain. Spectral metrics, calculated on the RRSS of the received Beacon frames, are like "snapshots" of the channel taken in a regular and periodical way and the classification uses properly selected features that measure the changes of consecutive "snapshots".

3. THE WIBECAM SYSTEM

The high-level architecture of the WIBECAM system is shown in Fig. 2. The first step is the collection of the RRSS from IEEE802.11b Beacon messages. We developed

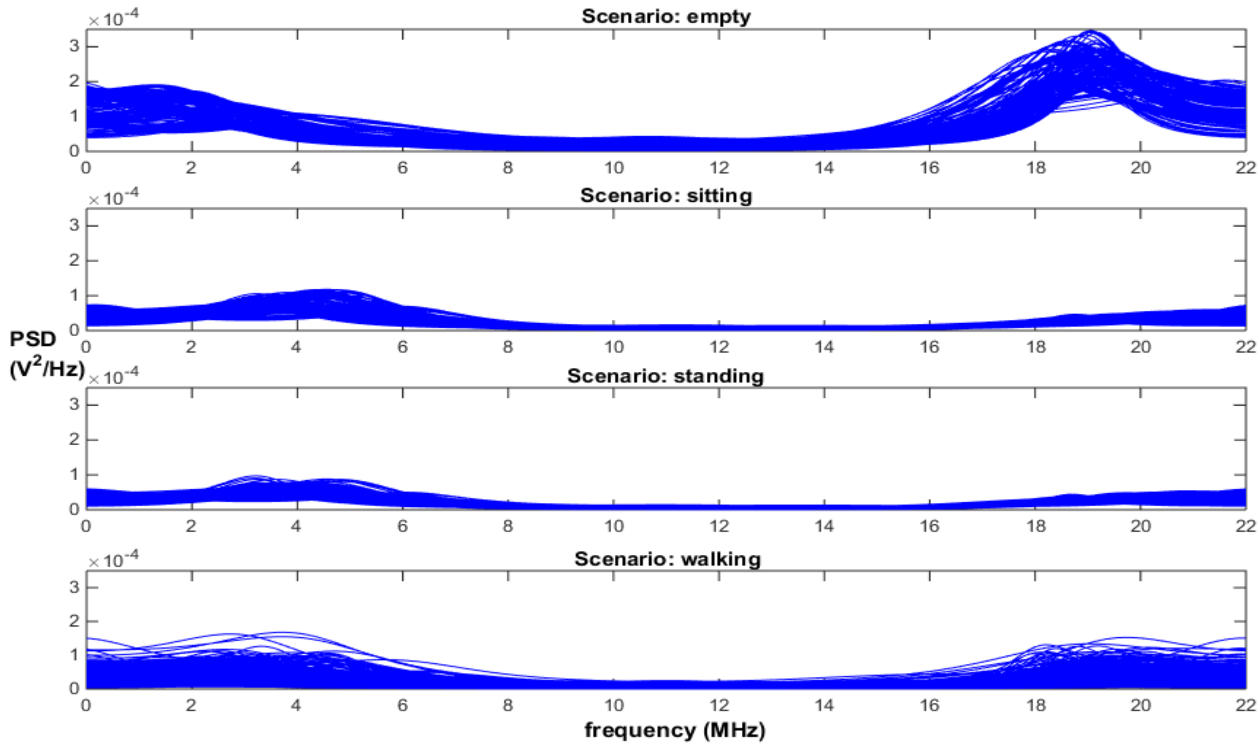

Figure 1: PSD of the signal of Beacon messages for different activities of the person. In each subplot, the PSD of 200 consecutive Beacon messages are plotted for the same scenario.

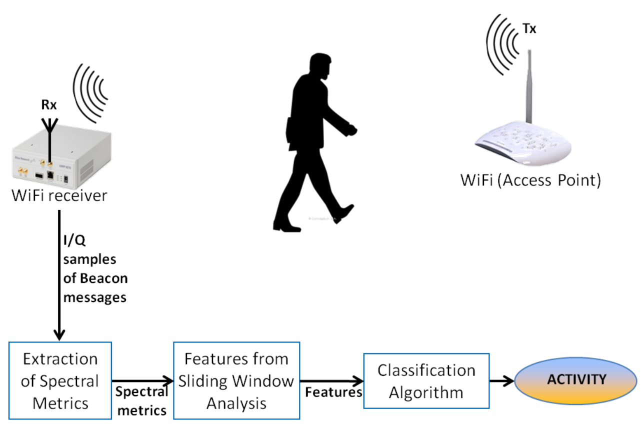

Figure 2: Block diagram of the proposed system.

an IEEE802.11b receiver using a Software Defined Radio (SDR) platform (Ettus N210), which collects the RRSS of the sequence of Beacons from one selected AP. The received signal has been sampled at $f_s = 22MHz$. Let us denote with $y^j(n)$, $0 \leq n \leq N-1$, the complex baseband representation of the samples, where $N = T_B f_s$ and T_B is the duration of one Beacon message. As it will be clarified in the next Subsection, it is important that the data content of each Beacon message is the same and hence, that we process the data transmitted by one specific AP. Therefore, the WIBECAM system stores the collected samples and then in parallel decode them to see which is the AP transmitting the received samples. If it is the one on which we are performing the AR, then, the stored samples are passed to the next processing box. Otherwise, the samples are discarded.

The second step is the extraction of the spectral metrics from the collected samples. As already mentioned, our AR system measures the difference of channel images in the frequency domain. In particular, over each Beacon message, the PSD $P^j(k)$ is computed. More precisely, WIBECAM computes the estimated PSD, $\hat{P}^j(k)$, through the autoregressive PSD estimate using the Yule-Walker method with a 3rd-order autoregressive model. This technique involves a fitting of the observations to the autoregressive model which is useful for the purpose of analyzing the shape of the spectrum since it smooths random peaks and pits while being sensitive to spectral shifts. This is particularly important for quantifying commonalities and differences between spectra while ignoring noisy fluctuations. Figure 1 shows $\hat{P}^j(k)$ for different activities, i.e. empty room, sitting, standing, walking. In each subplot, the PSD estimate of 200 consecutive Beacon messages are plotted for the same scenario. From Figure 1 it is evident that the shape of the PSD is affected by the type of activity. Therefore, the classification process of the WIBECAM system will be based on single-valued metrics related to the PSD shape, i.e. "images" of the channel) but also PSD distance metrics between consecutive "images" (to catch the time-variability due to the person's activity). In particular, the classification will be based on: the coefficient of variation of the spectral symmetry, the spectral Manhattan distance (mean and coefficient of variation) and the spectral Chebyshev distance (mean and coefficient of variation).

It is worth noting, that these metrics have been selected using the Sequential Forward Selection (SFS) algorithm, which has considered several other metrics, always related to the shape and the distance of consecutive PSD estimates, as specified in Subsection 3.2. Finally, the mentioned features are processed by a linear discriminant analysis classifier.

3.1 Theoretical Background

WIBECAM exploits the "multipath propagation" to perform AR. Due to multipath propagation, which is dominant in indoor environments, the received signal is a combination of different replicas of the transmitted signal, scattered from and reflected off different objects. In the time domain, this phenomena causes a time-dispersion of the signal energy (characterized by the so-called delay spread). The same phenomena seen in the frequency domain causes the channel to be frequency selective, meaning that different frequencies are attenuated differently. Moreover, in general the channel also varies over time. Let us model the channel as a linear system characterized by an equivalent lowpass time-varying impulse response $h(t, \tau)$, where t takes into account the time-variability of the channel and τ takes into account the frequency selectivity of the channel (τ describes the time-dispersion caused by the multipath). Let us denote with $x(t)$ the transmitted signal and $u(t)$ its complex envelope. If $y(t)$ is the baseband representation of the received signal, then $y(t) = (h * u)(t) = \int_{-\infty}^{\infty} h(t, \tau)u(t - \tau)d\tau$. At the receiver, both the real part and imaginary part of $y(t)$ are sampled at frequency f_s. If T_B is the duration of one Beacon message, let us consider the $N_s = T_B f_s$ samples of the complex representation of the received signal for the j-th Beacon message $y^j(n)$. We extract the behavior of the channel in the frequency domain by performing either a DFT or estimating the PSD over these samples. It is worth noting that the samples $y^j(n)$ contain both the channel ($h(t, \tau)$) and the data transmitted in the Beacon ($u(t)$). However, the AR process is based on the characterization of the "changes" among different images of the channel in the frequency domain, taken in one Beacon message. Therefore, if the data information contained by each Beacon message is the same, the changes between consecutive curves achieved by transforming in the frequency domain the Beacon sequence $y^j(n)$ are only related to the changes caused to the channel by the presence and activity of the person.

3.2 Spectral Metrics

The general idea is to characterize the channel in the frequency domain with curves and to define metrics that are related to the shape of these curves and to their changes over the time. The characterization of the channel in the frequency domain might be done by computing the N-points DFT $Y^j(k)$ or the PSD $P^j(k)$ of the received signal for the j-th Beacon message. Let us denote with $\phi^j(k)$ the complex magnitude of the DFT $Y^j(k)$ of the j-th Beacon ($\phi^j(k) = |Y^j(k)|$), or alternatively, the PSD estimate $\hat{P}^j(k)$ of the j-th Beacon ($\phi^j(k) = \hat{P}^j(k)$) using the Yule-Walker method with a m-th order autoregressive model.

For characterizing the "shape" of $\phi^j(k)$, symmetry, flatness and range might be used. Therefore, we have initially considered the following metrics:

Spectral Symmetry S^j:

$$S^j = \sum_{i=0}^{\lfloor N/2 \rfloor} |\phi^j(\lfloor N/2 \rfloor + i) - \phi^j(\lfloor N/2 \rfloor + 1 - i)| \quad (1)$$

Spectral Flatness F^j:

$$F^j = \frac{\sqrt[N]{\prod_{k=0}^{N-1} \phi^j(k)}}{\frac{1}{N}\sum_{k=0}^{N-1} \phi^j(k)} \quad (2)$$

Spectral Range R^j:

$$R^j = \max_k \phi^j(k) - \min_k \phi^j(k) \quad (3)$$

Furthermore, we have considered also several metrics related to the normalized distance between the spectra of two consecutive Beacon messages. It is worth noting that normalization is required since, as shown in Figure 1, the difference between spectral curves of the same scenario is sensitive to the average spectral power. In particular, it is evident that the human presence and activity decreases the average PSD. This is especially evident if we move from *sitting* to *standing* and to *walking*. Therefore, if we consider a distance metric between two PSD/DFT curves normalized to the mean, then this normalized distance increases from *empty* to *walking*, thus providing us with a better metric.

In the following, we provide the mathematical definition of spectral distance metrics:

Spectral Euclidean Distance R^j:

$$D_e^j = \frac{d_e(\phi^j(k), \phi^{j-1}(k))}{m(\phi^j(k)) \cdot m(\phi^{j-1}(k))} \quad (4)$$

where the function $d_e(\mathbf{a}, \mathbf{b})$ is the Euclidean distance between two vectors $\mathbf{a}$ and $\mathbf{b}$ and $m(\mathbf{a})$ is the sample mean of vector $\mathbf{a}$.

Spectral Manhattan Distance R^j:

$$D_M^j = \frac{d_M(\phi^j(k), \phi^{j-1}(k))}{m(\phi^j(k)) \cdot m(\phi^{j-1}(k))} \quad (5)$$

where the function $d_M(\mathbf{a}, \mathbf{b})$ is the Manhattan distance between two vectors $\mathbf{a}$ and $\mathbf{b}$.

Spectral Chebyshev Distance R^j:

$$D_C^j = \frac{d_C(\phi^j(k), \phi^{j-1}(k))}{m(\phi^j(k)) \cdot m(\phi^{j-1}(k))} \quad (6)$$

where the function $d_C(\mathbf{a}, \mathbf{b})$ is the Chebyshev distance between two vectors $\mathbf{a}$ and $\mathbf{b}$.

Spectral Decorrelation R^j:

$$D_d^j = \frac{d_d(\phi^j(k), \phi^{j-1}(k))}{m(\phi^j(k)) \cdot m(\phi^{j-1}(k))} \quad (7)$$

where $d_d(\mathbf{a}, \mathbf{b}) = \frac{1}{max(c(\mathbf{a}, \mathbf{b}))}$, and $c(\mathbf{a}, \mathbf{b})$ is the cross-correlation function between two vectors $\mathbf{a}$ and $\mathbf{b}$.

In addition, the RSS has been computed using the raw signal samples $y^j(n)$ as follows:

$$RSS^j = \frac{1}{N} \sum_{k=0}^{N-1} \|y^j(n)\|^2 \quad (8)$$

RSS has been computed as a reference metric since many works adopt this metric [9], [10], [11]. However, as it will be shown in the following, the SFS algorithm discard this metric, while it selects our metrics of shape and distance.

3.3 Video-camera Like Catching of the Time Variation

The videocamera-like approach that we follow in the present work foresees the evaluation of the difference between the channel "images". This is done by performing the statistical analysis through the statistical moments of order higher than 1 for spectral symmetry, spectral flatness and spectral range which are: sample standard deviation $\sigma(\cdot)$, coefficient of variation $c_v(\cdot)$, 3-rd sample moment $m_3(\cdot)$ and 4-th sample moment $m_4(\cdot)$. However, the metrics of spectral distance are implicitly defined as metrics of difference between channel "images", hence, for the metrics of spectral distance we will also consider the statistical moment of order 1, i.e. sample mean $m(\cdot)$. These statistical parameters are computed for the previously defined features over W Beacon message sequences $y^j(n)$ with a rolling window approach.

As it will be shown in the experimental results, the choice of the rolling window size W will greatly impact the performance of the classification. It is also intuitive that choosing a larger window size will help in increasing the recognition accuracy (correct classification rate), but this will increase the recognition delay which might be also an important performance parameters in some applications.

3.4 Feature Selection and Classification Algorithm for Activity Recognition

To choose the most informative features and the best combination of features, the SFS algorithm with 10-fold cross validation was used. This algorithm selects a subset of features that best predicts the activities by sequentially selecting features until there is no improvement in correct classification rate. The features analyzed by the SFS algorithm include all the spectral metrics previously defined (i.e. flatness, symmetry, range, normalized distance), computed using both DFT and PSD estimation for a variable number of points. Mean, coefficient of variation, 3-rd and 4-th central moment of RSS were also included within the overall set of features. The SFS algorithm has selected the following features: i) Coefficient of variation of spectral symmetry $\sigma(S)$); ii) Mean of spectral Manhattan distance $m(D_M)$; iii) Coefficient of variation of spectral Manhattan distance $\sigma(D_M)$; iv) Mean of spectral Chebyshev distance $m(D_C)$; v) Coefficient of variation of spectral Chebyshev distance $\sigma(D_C)$.

As a result of the feature selection process, we can state that:

- The PSD estimate is more suited than DFT.
- The PSD estimation based on the Yule-Walker method with a 3-rd order autoregressive model provided the best accuracy.
- The optimal number of points for the PSD estimation is small ($N = 256$) compared to the number of signal samples for each Beacon message ($N_s = 46815$).
- RSS provides lower accuracy with respect to spectral features.

For the classification task we utilized an algorithm based on linear discriminant analysis that fits a multivariate normal density to each class/activity, with a pooled estimate of covariance. This classification algorithm may not the best classification method, however, it is well suited for feature comparison.

4. EXPERIMENTAL RESULTS

We have carried out the experiments considering four different scenarios: 1) an empty room; 2) one person sitting; 3) one person standing; 4) one person walking. The activities have been carried out in different positions within the sensed room, as the AR must be independent from the specific position of the person performing the activities.

For each scenario we modified the configuration of the experiment in three different ways: a) modifying the position of the person sitting or standing and the pattern of the person walking; b) modifying the location of the AP and the receiver (Location A and B); c) considering two different office rooms (room I and II). Room I and II are different in size and in furniture. Location A refers to a line-of-sight (LOS) link between the AP and the receiver, while Location B refers to a non-line-of-sight (NLOS) link. In any configuration of the experiment, the distance between the monitored person and the AP or the receiver is higher than 2 m. The results of the WIBECAM system are presented in terms of confusion matrix for every configuration of the experiment and for two different values of the rolling window size: $W = 50$ and $W = 100$. Table 1 and 2 show the confusion matrix for Room I, Location A, achieved for $W = 50$ and $W = 100$ respectively. Table 3 and 4 presents the results for Location B. Table 5 and 6 show the confusion matrix for Room II, Location A, achieved for $W = 50$ and $W = 100$ respectively. Table 7 and 8 presents the results for Location B. First of all, these results prove the effectiveness of the proposed approach. In fact the accuracy ranges from a minimum of 0.73 to a maximum of 1, which seems a promising result compared to recent works (e.g. [12]). Second, we note that the lowest overall accuracies are achieved for NLOS configurations (Location B in both cases). Moreover, as expected, accuracy increases for longer rolling window size W. The dataset containing the selected features for each Beacon message has been divided into a training set (50%) and a test set (50%). The classifier has been trained separately for each configuration of the experiment (office room and position of the AP and receiver), but it is trained independently from the position where the activity is carried out. Therefore, the results are generalized in terms of position of the persons, but can not be generalized for different environments.

5. CONCLUSION

There are many device-free activity recognition systems based on RF signal analysis. Is there room for further new approaches? We present WIBECAM, an RF-based device-free activity recognition system which exploits three main concepts: 1) the RF signal is captured for WiFi Beacon messages only; 2) raw signal samples are collected and analyzed in the frequency domain using PSD estimation since it smooths random peaks and pits while being sensitive to spectral shifts; 3) a videocamera-like approach is followed for activity recognition, where our "images" are the PSD estimates and the difference between consecutive images is measured by using metrics of curve shape variation and distance between curves. A feature selection algorithm has been used to select a subset of features for classification purposes. In particular, the selected features from PSD estimates are: coefficient of variation of spectral symmetry, spectral Manhattan distance (mean and coefficient of variation), spectral Chebyshev distance (mean and coefficient of variation). Finally, a classification algorithm is applied to recognize the activity. Experiments have been carried out with different settings: two different office rooms, two different positions/patterns of the person; two different positions of the AP and receiver. The results prove the effectiveness of the WIBECAM approach, achieving overall accuracies ranging from 0.73 to 1 in different environments.

6. REFERENCES

[1] Y. Wang, J. Liu, Y. Chen, M. Gruteser, J. Yang, H. Liu, *E-eyes: Device-free Location-oriented Activity Identification Using Fine-grained WiFi Signatures*, 20th Int. Conf. on Mobile computing and networking (Mobicom '14), pp. 617-628, Sept. 7-11, 2014.

[2] J. Xiao, K. Wu, Y. Yi, L. Wang, L. M. Ni, *FIMD: Fine-grained Device-free Motion Detection*, 18th IEEE Int. Conf. on Parallel and Distributed Systems (ICPADS 2012), 2012.

[3] Chunmei Han, Kaishun Wu, Yuxi Wang, Lionel M. Ni, *WiFall: Device-Free Fall Detection by Wireless Networks*, IEEE Conf. on Computer Communications (IEEE INFOCOM 2014), April 27 2014-May 2 2014.

[4] Q. Pu, S. Gupta, S. Gollakota, S. Patel, *Whole-Home Gesture Recognition Using Wireless Signals*, 19th Int. Conf. on Mobile Computing and Networking, 2013.

[5] Moustafa Youssef, Matthew Mah, Ashok Agrawala, *Challenges: Device-Free Passive Localization for Wireless Environments*, 13th Int. conf. on Mobile computing and networking (Mobicom '07), pp. 222-229, 2007.

[6] F. Colone, P. Falcone, C. Bongioanni, P. Lombardo, *WiFi-Based Passive Bistatic Radar: Data Processing Schemes and Experimental Results*, IEEE Trans. on Aerospace and Electronic Sys., 48(2), 2012.

[7] Zheng Yang, Zimu Zhou, Yunhao Liu, *From RSSI to CSI: Indoor Localization via Channel Response*, ACM Computing Surveys (CSUR) Journal, vol. 46, no. 2, November 2013.

[8] Daniel Halperin, Wenjun Hu, Anmol Sheth, David Wetherall, *Predictable 802.11 Packet Delivery from Wireless Channel Measurements*, ACM SIGCOMM 2010 conference, pp 159-170, October 2010.

[9] Dian Zhang, Jian Ma, Quanbin Chen, Lionel M. Ni, *An RF-Based System for Tracking Transceiver-Free Objects*, IEEE PerCom 2007, pp. 135-144.

[10] A. E. Kosba, A. Saeed, M. Youssef, *RASID: A Robust WLAN Device-free Passive Motion Detection System*, IEEE Int. Conf. on Pervasive Computing and Communications (PerCom), 2012.

[11] S. Sigg, U. Blanke, G. Troester, *The Telepathic Phone: Frictionless Activity Recognition from WiFi-RSSI*, IEEE Int. Con. on Pervasive Computing and Communications (PerCom), Budapest, Hungary, March 24-28, 2014.

[12] S. Sigg, M. Scholz, S. Shi, Y. Ji, M. Beigl, *RF-Sensing of Activities from Non-Cooperative Subjects in Device-Free Recognition Systems Using Ambient and Local Signals*, IEEE Transactions on Mobile Computing, vol. 13, no. 4, April 2014.

[13] F. Adib, D. Katabi, *See Through Walls with Wi-Fi!*, SIGGCOM '13, August 12-16, 2013

	Prediction				
Truth	Empty	Sitting	Standing	Walking	
Empty	1	0	0	0	
Sitting	0.01	0.98	0.01	0	
Standing	0	0	1	0	
Walking	0	0.1	0.02	0.88	
					0.97

Table 1: Room I, Location A, W=50

	Prediction				
Truth	Empty	Sitting	Standing	Walking	
Empty	1	0	0	0	
Sitting	0	1	0	0	
Standing	0	0	1	0	
Walking	0.14	0.34	0	0.52	
					0.88

Table 2: Room I, Location A, W=100

	Prediction				
Truth	Empty	Sitting	Standing	Walking	
Empty	0.78	0.1	0.12	0	
Sitting	0.46	0.45	0	0.09	
Standing	0.04	0	0.96	0	
Walking	0	0.1	0.01	0.89	
					0.77

Table 3: Room I, Location B, W=50

	Prediction				
Truth	Empty	Sitting	Standing	Walking	
Empty	1	0	0	0	
Sitting	0.12	0.88	0	0	
Standing	0	0	1	0	
Walking	0	0	0	1	
					0.97

Table 4: Room I, Location B, W=100

	Prediction				
Truth	Empty	Sitting	Standing	Walking	
Empty	1	0	0	0	
Sitting	0	1	0	0	
Standing	0	0	1	0	
Walking	0	0	0	1	
					1

Table 5: Room II, Location A, W=50

	Prediction				
Truth	Empty	Sitting	Standing	Walking	
Empty	1	0	0	0	
Sitting	0	1	0	0	
Standing	0	0	1	0	
Walking	0	0	0	1	
					1

Table 6: Room II, Location A, W=100

	Prediction				
Truth	Empty	Sitting	Standing	Walking	
Empty	0.8	0.2	0	0	
Sitting	0	0.94	0.06	0	
Standing	0	0.27	0.73	0	
Walking	0	0.38	0.16	0.45	
					0.73

Table 7: Room II, Location B, W=50

	Prediction				
Truth	Empty	Sitting	Standing	Walking	
Empty	1	0	0	0	
Sitting	0	1	0	0	
Standing	0	0.03	0.97	0	
Walking	0.32	0.46	0.16	0.22	
					0.80

Table 8: Room II, Location B, W=100